

Type 1 Diabetes Management using GLIMMER: Glucose Level Indicator Model with Modified Error Rate

Saman Khamesian^{a,b,*}, Asiful Arefeen^{a,b}, Maria Adela Grando^a, Bithika M. Thompson^c, Hassan Ghasemzadeh^a

^aArizona State University, College of Health Solutions, Phoenix, 85004, AZ, USA

^bArizona State University, School of Computing and Augmented Intelligence, Tempe, 85281, AZ, USA

^cMayo Clinic Arizona, Department of Endocrinology, Scottsdale, 85259, AZ, USA

Abstract

Managing Type 1 Diabetes (T1D) demands constant vigilance as individuals strive to regulate their blood glucose levels to avert the negative consequences of dysglycemia (hyperglycemia or hypoglycemia). Despite the advent of sophisticated technologies such as automated insulin delivery (AID) systems, achieving optimal glycemic control remains a formidable task. AID systems integrate continuous subcutaneous insulin infusion and continuous glucose monitors (CGM) data, offering promise in reducing variability and improving glucose time-in-range. However, these systems often fail to prevent dysglycemia, partly due to limitations in prediction algorithms that lack the precision to prevent abnormal glucose events. This gap highlights the need for more advanced forecasting methods. We address this need with *GLIMMER*, Glucose Level Indicator Model with Modified ErroR Rate, a machine learning approach for forecasting blood glucose levels. GLIMMER categorizes glucose values into normal and abnormal ranges and devises a novel custom loss function to prioritize accuracy in dysglycemic regions where patient safety is critical. To evaluate the potential of GLIMMER for T1D management, we both use a publicly available dataset and collect new data involving 25 patients with T1D. In predicting next-hour glucose values, GLIMMER achieved a root mean square error (RMSE) of 23.97 (± 3.77) and a mean absolute error (MAE) of 15.83 (± 2.09) mg/dL. These results reflect a 23% improvement in RMSE and a 31% improvement in MAE compared to the best-reported error rates.

Keywords: Glucose Level Forecasting, Automated Insulin Delivery, Type 1 Diabetes, Machine Learning.

1. Introduction

Type 1 diabetes (T1D) is an autoimmune condition characterized by the destruction of insulin-producing beta cells in the pancreas, leading to a lifelong dependency on exogenous insulin. Managing T1D is particularly challenging due to the need for continuous monitoring and precise insulin dosing to maintain blood glucose levels within a target range. Poor glucose control can lead to severe complications, including cardiovascular diseases, neuropathy, retinopathy, and kidney failure [1, 2, 3]. As a result, effective diabetes management is crucial for enhancing quality of life and reducing the long-term complications associated with T1D. Furthermore, it is estimated that around 8.4 million people worldwide suffer from T1D, representing approximately 5-10% of all diabetes cases [4]. The prevalence of T1D varies significantly across different populations and regions, highlighting the importance of tailored management strategies to address the unique needs of patients globally.

Predicting future blood glucose levels is crucial for preventing dangerous dysglycemic events (hypoglycemia and hyperglycemia) and supporting timely, proactive interventions focused on medication dosing

*Corresponding author.

Email address: skhamesi@asu.edu (Saman Khamesian)

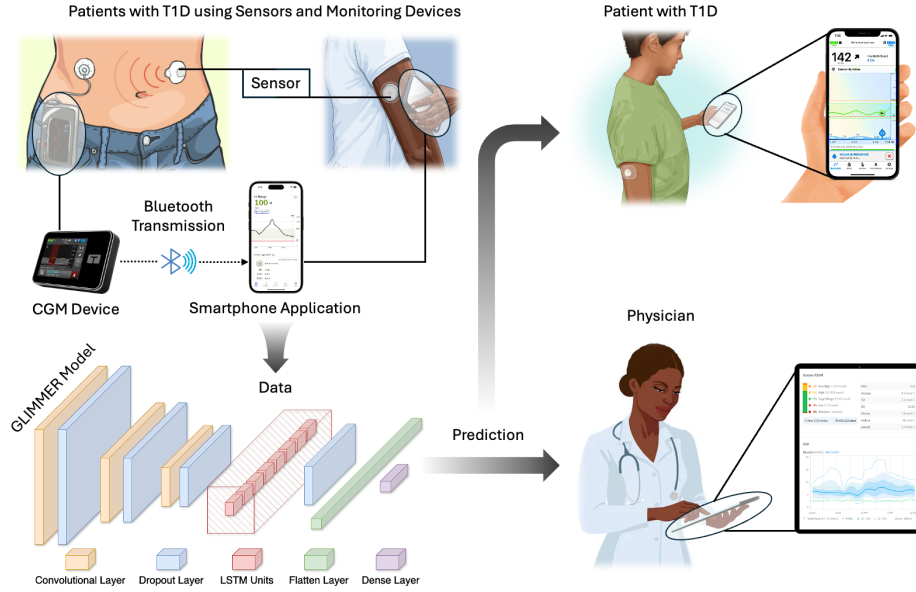


Figure 1: GLIMMER’s application in a T1D management system integrates with sensor technology, where data is sent directly to a smartphone or transmitted from a CGM device via Bluetooth or other methods. The data is then processed and used as input to the GLIMMER model, which predicts the next hour of glucose levels and reports potential dysglycemic events. This helps patients manage their condition more effectively and supports physicians in making informed treatment decisions.

and behavioral modifications. Errors in these critical regions carry serious health risks, whereas deviations within the normal range are generally less impactful [5, 6]. Long-term predictions, such as those extending beyond the more common 15–30 minute horizon to 60 minutes or longer, offer patients and clinicians greater lead time to respond effectively, enhancing safety and reducing stress [7, 8, 9]. When embedded in technologies like automated insulin delivery (AID) and hybrid closed-loop (HCL) systems, robust prediction models can help overcome the physiological delays of insulin action and glucose sensing, allowing for earlier alerts or therapeutic adjustments before glucose levels enter dangerous ranges [10, 11, 12].

Despite advancements in diabetes management technologies, several limitations persist. Existing glucose prediction models often rely on generic architectures and overlook the domain-specific complexities of 1 T1D management. Many models fail to maintain accuracy in clinically significant dysglycemic regions, particularly during rapid fluctuations such as postprandial glucose spikes, where timely intervention is critical. AID systems, which rely heavily on these forecasts, often struggle to predict and react quickly enough to post-meal rises, leading to corrective boluses that are delayed or insufficient [13, 14]. Another key challenge lies in data availability: the high cost and burden of collecting detailed, labeled data limit access to large, high-quality datasets [15]. This creates a cold-start problem for researchers and hinders model generalizability and personalization [16].

To address these challenges, we propose **GLIMMER**¹ (Glucose Level Indicator Model with Modified Error Rate), a domain-specific prediction framework designed for T1D management. Our approach uniquely combines tailored feature engineering, extensive hyperparameter tuning, and a novel custom loss function that prioritizes accuracy in clinically critical (dysglycemic) regions—an objective not addressed by prior studies. This loss function places greater weight on errors during hyperglycemic and hypoglycemic events, enabling the model to more effectively anticipate postprandial glucose spikes and support earlier corrective actions. These improvements directly address a major limitation of current AID systems, which often respond too slowly or deliver insufficient insulin after meals [13, 14].

¹<https://github.com/SamanKhamesian/GLIMMER>

To overcome the limitations of existing datasets, we also conducted a real-world study in collaboration with Mayo Clinic Arizona and introduced the **AZT1D** [17]², a dataset comprising 26,707 hours of multi-modal data from 25 patients with T1D. GLIMMER demonstrates superior forecasting performance even at extended prediction horizons (60 minutes), achieving a 23% improvement in RMSE and a 31% improvement in MAE on the OhioT1DM dataset, and generalizes effectively to the AZT1D dataset. We illustrate its potential integration into clinical workflows in Figure 1.

2. Related Work

Machine learning and deep learning approaches have significantly advanced blood glucose prediction, enabling proactive interventions and improved glycemic control for patients with T1D. Marigliano et al. [8] demonstrated that integrating predictive alarms with CGM technology reduced hypoglycemic events in adolescents by 40% and severe hypoglycemia by 60%, highlighting the clinical benefits of early warnings. Similarly, Vettoretti et al. [9] showcased how artificial intelligence-based management systems can improve outcomes by prompting timely interventions such as insulin dose adjustments or dietary changes. Building on this idea, Shroff et al. [18] proposed a personalized prediction system that learns individual response patterns and provides tailored alerts, shifting diabetes care from reactive to proactive. In line with these efforts, Arefeen et al. [19] developed machine learning algorithms to predict postprandial hyperglycemia using data from controlled feeding trials.

To further improve prediction capabilities, researchers have explored more sophisticated architectures such as Convolutional Recurrent Neural Networks (CRNN) [20], which estimate glucose levels for up to a 60-minute prediction horizon (PH) based on prior CGM data and information on meal and insulin intakes. Li et al. [21] introduced this model, combining the feature extraction capabilities of convolutional neural networks (CNN) [22] with the temporal learning capabilities of recurrent neural networks (RNN) [23]. The CRNN demonstrated superior performance in both simulated and real patient data, providing accurate short-term glucose predictions essential for proactive diabetes management.

Along similar lines, Long Short-Term Memory (LSTM) [24] networks have also been employed to capture long-term dependencies in glucose trends. Aliberti et al. [25] developed a predictive model using a multi-patient dataset and demonstrated that LSTM networks significantly outperformed Non-Linear Autoregressive (NAR) neural networks [26] in both short- and long-term predictions. This improvement is attributed to LSTM’s ability to handle long-term dependencies and mitigate issues like the vanishing gradient problem, underscoring its potential to enhance predictive accuracy and clinical outcomes for diabetes management. Building upon LSTM networks, bi-directional variants have been explored to further improve predictions by considering both past and future data points. Sun et al. [27] applied bi-directional LSTM networks for glucose prediction, while Butt et al. [28] investigated how feature transformation techniques can enhance the efficiency of such models. These approaches provide a more comprehensive understanding of glucose trends and lead to improved prediction accuracy.

In contrast to deep learning methods, linear regression remains a simple yet effective approach in commercial systems. The Tandem t:slim X2 with Control-IQ technology, for example, employs linear regression to forecast glucose levels 30 minutes ahead based on previous CGM data. To address the limitations of linear regression in time-series and multi-step predictions, Zhang et al. [29] developed a multiple linear regression (MLR) model that predicts each future time step separately. Despite the challenges of using linear regression for time-series forecasting, the structured MLR approach improves prediction accuracy at various horizons, thereby enhancing the reliability of automated insulin delivery systems.

While these studies have considerably advanced prediction accuracy and clinical utility, many rely on generic architectures without clear justification of design choices or incorporation of domain-specific features such as meal timing or physical activity. Furthermore, most models optimize for mean prediction error and overlook the clinical importance of minimizing errors in hypo- and hyperglycemic regions [6, 8]. A summary of these models, their main characteristics, and their limitations is presented in Table 1, illustrating the need for a domain-specific, clinically-focused approach.

²<https://data.mendeley.com/datasets/gk9m674wcx/1>

Table 1: Summary of Related Models in Blood Glucose Forecasting

Model	Key Features	Limitations
FCNN [16]	Fully-connected neural network; simple, fast, easy to train.	Lacks the ability to capture temporal dependencies important for glucose trends.
CNN [30]	Local pattern extraction via convolutions; low latency.	Limited in modeling long-term dependencies; emphasizes mean error rather than clinically relevant regions.
CRNN [21]	Combines CNN and RNN to capture local & temporal patterns.	Limited attention to dysglycemic regions; general-purpose architecture without domain-specific enhancements.
Bi-LSTM [27]	Uses past and future context for improved sequence modeling.	Computationally intensive; does not incorporate domain-specific loss optimization.
GRU [31]	Faster and lighter than LSTM; good for medium-range dependencies.	Less effective at modeling long sequences; prioritizes mean error over critical glucose regions.
Transformer [32]	Attention-based; models long-range dependencies; handles multimodal inputs.	Requires large datasets; does not explicitly focus on hypo- and hyperglycemic regions.
ARIMA [33]	Linear autoregressive; interpretable baseline.	Limited in modeling nonlinear, multimodal, and long-term dynamics.
MLP [34]	Simple shallow network; fast inference of basic non-linear patterns.	Lacks capacity to model sequential dependencies and specific glucose dynamics.

3. Methodology

3.1. Model Architecture

The decision to use a CNN-LSTM model for GLIMMER is motivated by its hybrid architecture, which combines the automatic feature extraction capabilities of convolutional layers with the temporal modeling strengths of LSTM units [22, 24]. CNNs capture spatial relationships within multivariate physiological data, while LSTMs are well-suited for learning sequential patterns and long-term dependencies. This integration enables the model to uncover hidden features and capture abrupt changes in CGM trends, making it highly effective for blood glucose forecasting. Recent work by Jaloli and Cescon (2023) [7] demonstrated that CNN-LSTM outperforms LSTM, CRNN, and other models in both predictive accuracy and clinical relevance, especially over longer prediction horizons. Similar success has been observed in other time-series domains such as stock forecasting, energy load prediction, and wind power estimation [35, 36, 37]. To find the most suitable parameters for the CNN-LSTM architecture, we designed an experiment to analyze and identify the optimal configuration, with the fine-tuning process detailed in Section 5.1.

3.2. Custom Loss Function

Glucose values are typically divided into three clinically meaningful regions: hypoglycemia, normal, and hyperglycemia as shown in (1). Values below the hypoglycemia threshold T_{hypo} indicate dangerously low glucose levels, while values above the hyperglycemia threshold T_{hyper} indicate excessively high levels. Measurements that fall between these two thresholds are considered within the normal range. In practice, T_{hypo} and T_{hyper} are often set to 70 mg/dL and 180 mg/dL, respectively, based on guidelines and prior studies [38, 8, 9]. Prediction errors in the critical regions of hypo- and hyperglycemia are particularly dangerous for patients with T1D, as they can lead to missed interventions and serious complications. Woldaregay et al. [5] highlighted that prior studies rarely account for the uneven clinical impact of such errors.

To address this gap, we propose penalizing prediction errors more heavily in critical regions than in the normal range. Figure 2 is an example of CGM readings data that highlights the regions and thresholds.

$$\text{Glucose Level Regions} = \begin{cases} 1, & x < T_{hypo} \\ 2, & T_{hypo} \leq x \leq T_{hyper} \\ 3, & x > T_{hyper} \end{cases} \quad (1)$$

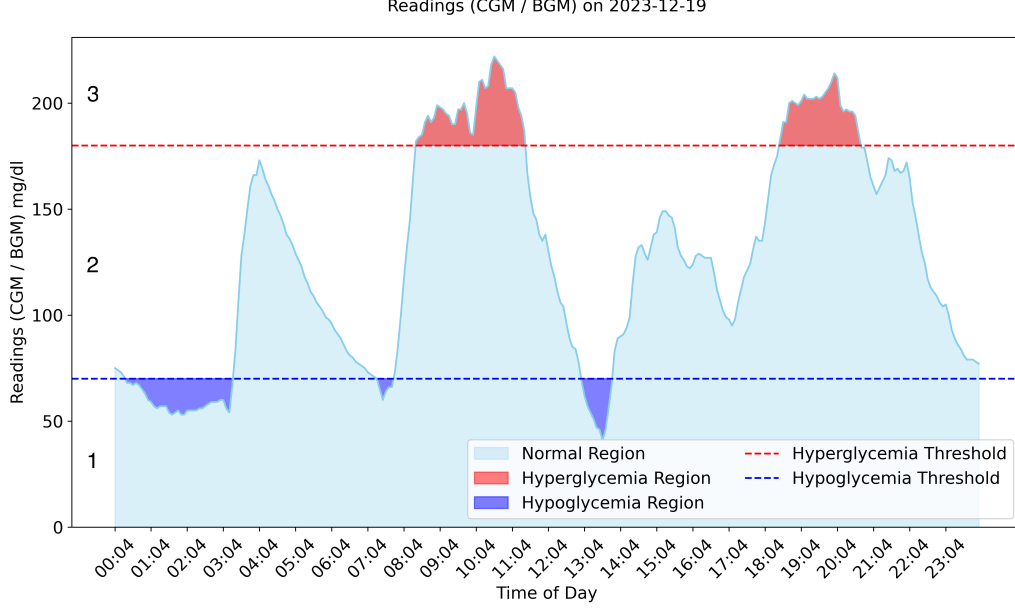


Figure 2: CGM readings from a patient in the AZT1D dataset on December 19, 2023, showing blood glucose fluctuations over 24 hours. Regions are labeled as follows: (1) Hypoglycemia (below 70 mg/dL, blue), (2) Normal range, and (3) Hyperglycemia (above 180 mg/dL, red). Dashed lines indicate hypoglycemia (blue) and hyperglycemia (red) thresholds.

we then break down the total error, which represents the cumulative prediction error across all data points, into individual errors within each critical region. By applying specific weights to these errors, our approach ensures that the model is more sensitive to inaccuracies where they matter most, enhancing its reliability and effectiveness in managing T1D. This total error, which we compute as the summation of individual losses, can be formalized as shown in (2):

$$Error_{total} = \sum_{i=1}^3 w_i \times Error_i \quad (2)$$

The total error serves as the model’s loss function aggregated over all instances, enabling it to capture and prioritize prediction accuracy within distinct regions. If we choose Mean Absolute Error (MAE) as the error term $Error_i$, and assign weights w_{hypo} , w_{normal} , and w_{hyper} to the hypoglycemia, normal, and hyperglycemia regions, respectively, the total error can be calculated as follows:

$$MAE = \frac{1}{N} \sum_{i=1}^N |y_i - \hat{y}_i| \quad (3)$$

$$Error_{total} = \frac{w_{hypo}}{n_1} \sum_{i=1}^{n_1} |y_i - \hat{y}_i| + \frac{w_{normal}}{n_2} \sum_{i=1}^{n_2} |y_i - \hat{y}_i| + \frac{w_{hyper}}{n_3} \sum_{i=1}^{n_3} |y_i - \hat{y}_i| \quad (4)$$

where n_1 , n_2 and n_3 represent the total number of blood glucose samples in each region, and y_i and \hat{y}_i represent the predicted value and true value of the glucose level, respectively. The main research question that remains to be answered is how to determine the parameters of this error equation, including weight and threshold values.

3.3. Error Weights

We classify CGM values into regions based on the thresholds discussed earlier. Next, we finalize the custom loss function by determining the optimal weights for each region, focusing on dysglycemia. To simplify optimization, we fix $w_{normal} = 1$, reducing the task to finding w_{hypo} and w_{hyper} . To find these weights, we use a Genetic Algorithm (GA) [39], a robust optimization method well-suited for problems where the fitness function involves training a model and evaluating its error. GAs require no derivatives or assumptions about the search space [39, 40, 41], and their flexibility makes them ideal for this task. In our implementation, the GA optimizes w_{hypo} and w_{hyper} for each patient by evolving a population of candidate weight pairs. This ensures the weights are adapted to the clinical relevance of each region and tailored to each patient. The procedure is as follows:

1. For each patient, initialize a random population of $N = 20$ weight pairs $w = [w_{hypo}, w_{hyper}]$, sampled uniformly from the range $[1, 10]$.
2. Repeat the following for $G = 25$ generations:
 - (a) Evaluate the fitness of each individual by training the model with its weights and computing the total prediction error on validation data.
 - (b) Select the top $N/2$ individuals with the lowest errors as parents.
 - (c) Generate $N/2$ offspring as follows:
 - i. Randomly select two parents and average their weights to create a child.
 - ii. Add Gaussian noise ($\mathcal{N}(0, 0.5)$) to the child weights to introduce variation.
 - iii. Clip the child weights to ensure they remain within $[1, 10]$.
 - (d) Form the next generation by combining the parents and offspring.
3. After G generations, select the weight pair with the lowest validation error as the optimal w^* .

In summary, our methodology combines three key components to enhance prediction performance: selecting a suitable model architecture, designing a custom loss function that emphasizes clinically critical regions, and using a genetic algorithm to tune the loss function’s weights. Figure 3 illustrates the complete methodology for the design and evaluation of GLIMMER. In the following sections, we describe the feature engineering that contributes to improved model performance, as well as the experiments conducted to determine the optimal CNN-LSTM architecture and custom loss function weights.

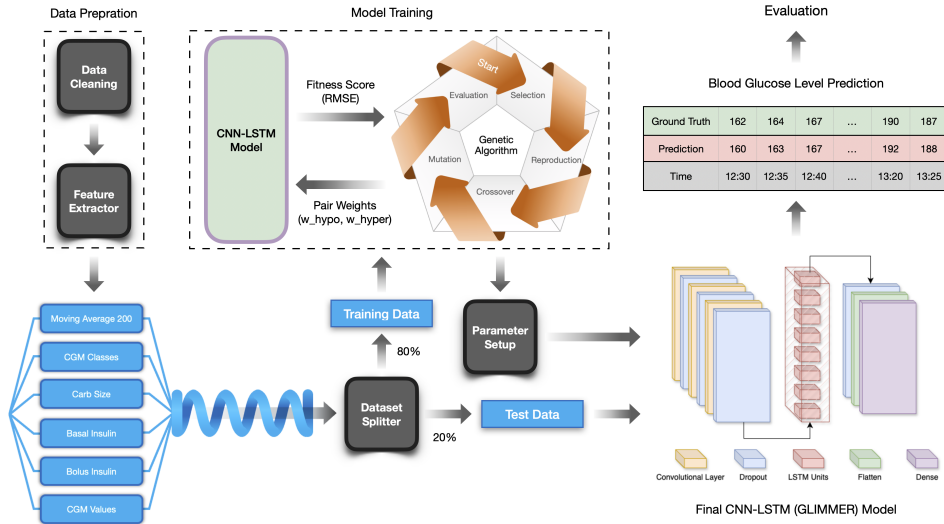


Figure 3: The proposed methodology in GLIMMER for predicting blood glucose levels in patients with T1D. CGM data undergo preprocessing and feature extraction before being split for training and testing. A genetic algorithm optimizes a custom loss function used to train the CNN-LSTM model, which is then evaluated on the test data using the finalized parameters.

4. Data

4.1. OhioT1DM Dataset

We utilized the OhioT1DM dataset [42], which includes data from 12 individuals with T1D. The dataset contains raw glucose values recorded every 5 minutes, along with basal insulin, bolus insulin, and carbohydrate intake over an 8-week period.

4.2. AZT1D Dataset

Alongside the OhioT1DM dataset, we introduced and published a new dataset named AZT1D [17]. We collected data from 25 patients with T1D using AID systems who visited the endocrinology clinic at the Mayo Clinic in Scottsdale, AZ, between December 2023 and April 2024 for their regular appointments. The participants included 13 females and 12 males, aged between 27 and 80 years, with an average age of 59 years. Informed consent was obtained from all participants under the study protocol (IRB #23-003065). For each patient, the dataset contains an average of 26 days of real-world recordings, including CGM signals captured with Dexcom G6 Pro, insulin logs, meal carbohydrate sizes, and device modes (regular/sleep/exercise) recorded from the Tandem t:slim X2 insulin pump. In total, the dataset comprises 320,488 CGM entries spanning approximately 26,707 hours of monitoring data.

4.3. Data Preparation

The OhioT1DM dataset consists of 24 files from 12 patients, with two files per patient: one for training and one for testing [42]. To avoid overfitting and to enable hyperparameter tuning, we further split the training file chronologically, using the first 80% for training and the remaining 20% for validation. The separate testing file is kept intact and used exclusively for final evaluation.

For the AZT1D dataset [17], which does not come pre-partitioned, we applied a similar strategy: each patient’s data was split into 80% for training and 20% for testing, and then the training portion was again split into 80% training and 20% validation.

In addition to CGM values, basal insulin, bolus insulin, and carbohydrate amounts, we crafted two additional features to enhance model performance. First, we computed the 200-period moving average of CGM values to smooth short-term fluctuations from meals, activity, or stress, allowing the model to focus on the long-term trend relevant for predictions [43, 44]. This trend emphasis reduces overfitting to transient spikes or drops. Second, we assigned each CGM value a class label (hypoglycemia, normal, hyperglycemia) based on thresholds, as detailed in Section 3, helping the model recognize clinically important ranges. In total, six input features were used in a sliding-window format (Figure 4).

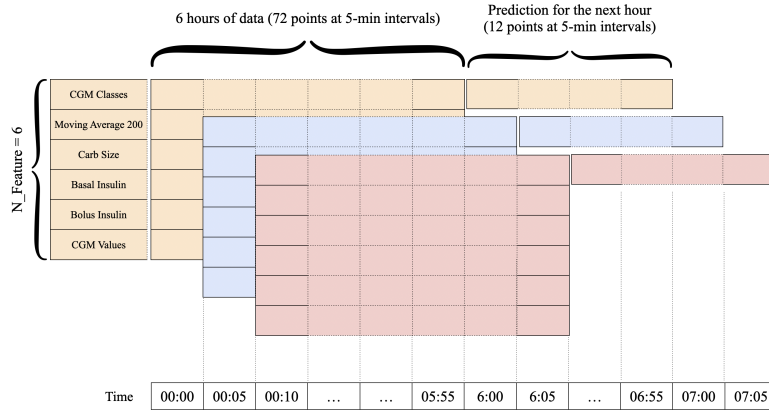


Figure 4: For time-series data, we treat it as sequential and use a sliding window to create samples for training a CNN-LSTM model. Since CGM values are recorded every five minutes, the window moves in five-minute steps, capturing both X (input) with 72 units and y (output) with 12 units. Each data unit includes 6 features. The figure above illustrates 3 data samples, each covering a 7-hour period.

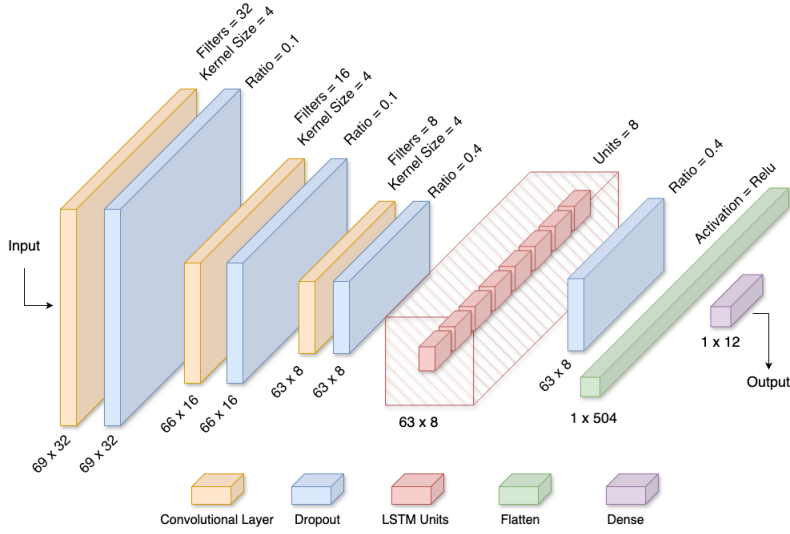


Figure 5: Diagram of the proposed CNN-LSTM architecture. The input consists of 6 hours of time-series data with 6 features each, while the output provides a 1-hour prediction of glucose levels.

5. Experimental Setup

5.1. Architecture Configuration

We reviewed previous studies to identify common configurations for CNN-LSTM models, which typically use 1–4 convolutional layers and 8–128 LSTM units [30, 45]. Guided by these insights, we designed an experiment to systematically evaluate different layer and unit configurations. We used a subset of the dataset, split into 80% for training and 20% for validation. The results of these experiments are summarized in Table 2. The final architecture, shown in Figure 5, consists of three 1D convolutional layers (kernel size 4; 32, 16, and 8 filters), an LSTM layer with 8 units, a flattening layer, and a dense layer with ReLU activation.

5.2. Custom Loss Function Parameters Configuration

We conducted an experiment using the genetic algorithm described in Section 3 to determine the optimal weights for our custom loss function. In each generation, the performance of each candidate was evaluated by applying its weights to the custom loss function, compiling, and running the CNN-LSTM model. The RMSE on the validation dataset was then computed and used as the fitness score. Through this process, we identified the best weights for each patient. However, calculating personalized weights for every patient is impractical in real-world settings due to the computational cost of running the genetic algorithm repeatedly. To address this, we computed the average weights across all patients, yielding $(w_{hypo}, w_{hyper}) = (3.296, 2.382)$. This averaged configuration offers a balanced solution that generalizes well while avoiding the inefficiencies of per-patient optimization, providing a practical approximation of the custom loss function’s performance.

Table 2: RMSE for CNN-LSTM Models with Various Configurations of Patient 559 from the OhioT1DM Dataset

Convolutional Layers	1 LSTM Layer				2 LSTM Layers			
	4 Units	8 Units	16 Units	32 Units	4 Units	8 Units	16 Units	32 Units
1 Layer (32 filters)	38.62	31.48	34.22	33.94	33.04	31.90	43.78	43.02
2 Layers (32 and 16 filters)	29.28	30.12	35.12	33.72	35.17	32.28	34.63	39.84
3 Layers (32, 16 and 8 filters)	28.86	28.54	29.01	28.84	28.85	30.57	30.6	38.39

5.3. Evaluation Metrics

To assess the performance of the GLIMMER model, we employed standard metrics commonly used in related studies [16, 21, 25, 28], including:

5.3.1. Root Mean Square Error (RMSE)

This metric provides insight into the average deviation of predicted values from actual values, with an emphasis on larger errors:

$$\text{RMSE} = \sqrt{\frac{1}{n} \sum_{i=1}^n (y_i - \hat{y}_i)^2} \quad (5)$$

Here, n represents the number of data points, y_i denotes the ground truth or actual CGM value, and \hat{y}_i is the predicted CGM value.

5.3.2. Mean Absolute Error (MAE)

This metric quantifies the average absolute difference between predicted and observed values, providing a straightforward interpretation of prediction accuracy. It is calculated as follows:

$$\text{MAE} = \frac{1}{n} \sum_{i=1}^n |y_i - \hat{y}_i| \quad (6)$$

5.3.3. Precision

This metric indicates the accuracy of the positive predictions made by the model, defined as the ratio of true positives (TP) to the sum of true positives and false positives (FP). It is calculated as:

$$\text{Precision} = \frac{TP}{TP + FP} \quad (7)$$

5.3.4. Recall

This metric reflects the model's ability to identify all relevant instances, representing the true positive rate. It is the ratio of true positives to the sum of true positives and false negatives (FN):

$$\text{Recall} = \frac{TP}{TP + FN} \quad (8)$$

5.3.5. F1 Score

The F1 score provides a balance between precision and recall, especially useful when dealing with imbalanced classes. It is calculated as:

$$\text{F1} = 2 \cdot \frac{\text{Precision} \cdot \text{Recall}}{\text{Precision} + \text{Recall}} \quad (9)$$

5.3.6. Clarke Error Grid Analysis

The Clarke Error Grid (CEG) analysis [46] is a widely accepted tool for evaluating the clinical accuracy of glucose predictions by comparing them to reference glucose values. It classifies predictions into five distinct regions, each representing varying levels of clinical significance:

- **Region A:** Includes values within 20% of the reference value, indicating clinically accurate predictions.
- **Region B:** Contains values outside of the 20% range but unlikely to result in inappropriate treatment.
- **Region C:** Identifies predictions that may lead to unnecessary treatment.
- **Region D:** Represents predictions where critical hypoglycemia or hyperglycemia might be missed.
- **Region E:** Captures predictions that could lead to confusion between treating hypoglycemia and hyperglycemia, a highly dangerous scenario.

6. Results

After data preparation and finalizing the GLIMMER model by setting up the parameters of the architecture and custom loss function, we conducted extensive experiments using a batch size of 48, over 30 epochs, with a prediction horizon (PH) of 60 minutes. To minimize the impact of randomness, we conducted 10 iterations of the experiments for each patient using a unique seed number for each run and reported the average results of these trials. All experiments were performed on an Apple M3 Pro chip featuring a 12-core CPU, an 18-core GPU, a 16-core Neural Engine, and 18 GB of unified memory.

6.1. Overall Performance

Tables 3 and 4 summarize the performance comparison of GLIMMER with other methods for the OhioT1DM and AZT1D datasets, both using a PH of 60 minutes. We selected the most recent studies that employed a variety of classical and machine learning models, including Fast-Adaptive and Confident Neural Network (FCNN) [16], CRNN [21], Bi-LSTM [27], transformer models [32], Random Forest Regression (RFR) [34, 16], Support Vector Regression (SVR) [47], and Autoregressive Integrated Moving Average (ARIMA) [33]. Additionally, we included the original GLIMMER model, implemented as a basic CNN-LSTM, to highlight the impact of our enhancements. These enhancements incorporate CGM region classes and moving averages as additional features, a custom loss function optimized with a genetic algorithm, improved architecture design, and tuned hyperparameters.

The results include RMSE and MAE, reported as (Mean \pm Standard Deviation), along with CEG metrics to assess prediction errors. Lower RMSE and MAE indicate better performance. As shown in Table 3, GLIMMER achieves a 23% improvement in RMSE and 31% in MAE compared to the best-reported errors. The basic CNN-LSTM also performs well, making it a viable option when other models are unsuitable. In the CEG analysis, higher values in Region A and lower in other regions are desirable. GLIMMER attains 85% in Region A, a 15% improvement over FCNN, while maintaining low values elsewhere.

Table 3: Prediction Performance Comparison on the OhioT1DM Dataset with PH = 60 minutes

Model Name	RMSE (mg/dL)	MAE (mg/dL)	CEG-Regions (%)				
			A	B	C	D	E
FCNN [16]	31.07 \pm 3.62	22.86 \pm 2.89	72.58 \pm 7.87	24.39 \pm 6.41	0.16 \pm 0.14	2.85 \pm 1.68	0.02 \pm 0.04
CRNN [21]	32.02 \pm 3.76	23.82 \pm 3.13	71.06 \pm 8.69	25.57 \pm 7.07	0.15 \pm 0.17	3.20 \pm 1.99	0.01 \pm 0.04
Bi-LSTM [27]	33.44 \pm 3.76	24.59 \pm 2.89	70.61 \pm 8.21	25.98 \pm 6.70	0.17 \pm 0.13	3.19 \pm 1.89	0.05 \pm 0.07
Transformer [32]	32.96 \pm 3.70	24.19 \pm 2.79	71.70 \pm 7.77	25.20 \pm 6.43	0.15 \pm 0.15	2.92 \pm 1.65	0.04 \pm 0.05
SVR [47]	33.83 \pm 3.62	25.63 \pm 2.98	66.43 \pm 9.15	29.61 \pm 7.30	0.20 \pm 0.21	3.73 \pm 2.62	0.03 \pm 0.04
RFR [34]	35.31 \pm 3.72	26.43 \pm 3.02	67.03 \pm 8.17	29.38 \pm 6.29	0.23 \pm 0.19	3.34 \pm 2.14	0.02 \pm 0.04
ARIMA [33]	35.42 \pm 3.74	25.97 \pm 2.70	68.77 \pm 6.85	28.65 \pm 5.83	0.46 \pm 0.40	2.06 \pm 1.00	0.05 \pm 0.05
Basic CNN-LSTM	31.98 \pm 4.15	23.00 \pm 2.87	74.31 \pm 7.03	23.12 \pm 5.96	0.11 \pm 0.14	2.43 \pm 1.56	0.03 \pm 0.08
GLIMMER	23.97 \pm 3.77	15.83 \pm 2.09	85.46 \pm 4.87	13.26 \pm 4.29	0.13 \pm 0.17	1.12 \pm 0.57	0.02 \pm 0.07

Table 4: Prediction Performance Comparison on the AZT1D Dataset with PH = 60 minutes

Model Name	RMSE (mg/dL)	MAE (mg/dL)	CEG-Regions (%)				
			A	B	C	D	E
Basic CNN-LSTM	29.55 \pm 6.49	21.61 \pm 5.19	73.27 \pm 8.57	24.47 \pm 7.65	0.03 \pm 0.07	2.21 \pm 1.67	0.02 \pm 0.05
GLIMMER	22.48 \pm 3.57	15.58 \pm 2.87	83.89 \pm 5.01	14.94 \pm 4.54	0.02 \pm 0.03	1.12 \pm 0.85	0.02 \pm 0.04

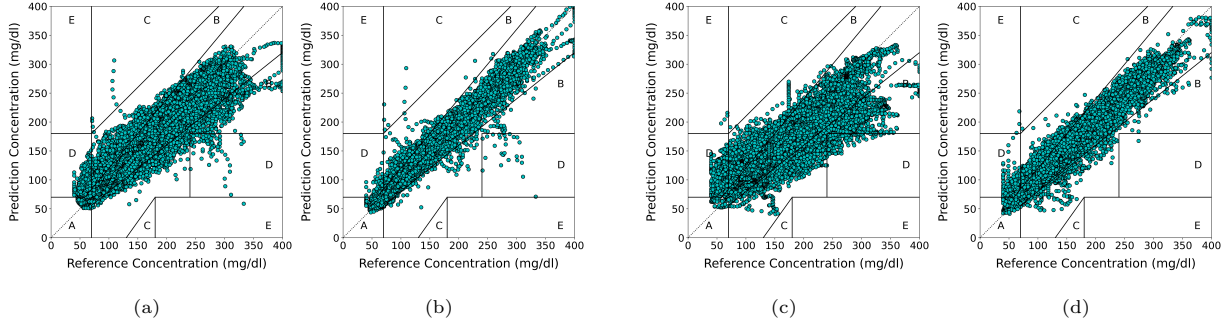


Figure 6: Clarke Error Grid for the basic CNN-LSTM model and GLIMMER across all patients. Figures a and b pertain to the OhioT1DM dataset (with a for the basic CNN-LSTM and b for GLIMMER), while figures c and d relate to the AZT1D dataset (with c for the basic CNN-LSTM and d for GLIMMER). The detailed percentages for each region are represented in Tables 3 and 4. In both datasets, the results are tightly clustered near the $x=y$ line, indicating that GLIMMER’s predictions are as close as possible to the reference values.

Table 4 shows results for GLIMMER and the basic CNN-LSTM on the AZT1D dataset. Again, GLIMMER outperforms the basic CNN-LSTM, with a 24% improvement in RMSE and 28% in MAE. Since this dataset is newly collected and not publicly available, we report results only for these two models, leaving broader comparisons to future work. Given the close results on the OhioT1DM dataset between CNN-LSTM and other models like FCNN and CRNN, similar trends are expected here.

To ensure a fair comparison, we excluded the MLR model from Table 3, as it requires training a separate model for each prediction horizon (PH). At a PH of 60 minutes, this entails 12 individual models for predicting the next 5, 10, \dots , up to 60 minutes. In contrast, the models in Table 3 use a single model for all horizons. Moreover, the MLR study did not report CEG results. While its RMSE (24.58 mg/dL) and MAE (17.42) surpass some models, GLIMMER still outperforms it.

Figure 6 visualizes the CEG analysis results for both the OhioT1DM and AZT1D datasets, complementing the numeric results reported in Tables 3 and 4. The plots compare the basic CNN-LSTM and the GLIMMER model across datasets, showing how predictions are distributed across the CEG regions. GLIMMER’s predictions are more concentrated in Region A and closer to the diagonal $x = y$ line, indicating better clinical accuracy and fewer large errors, particularly in critical regions. This visualization highlights GLIMMER’s improved ability to forecast blood glucose levels reliably, which is crucial for both clinical evaluation and practical deployment.

6.2. Regional and Event-Specific Performance

In our analysis, we calculated error metrics separately for normal glucose levels and dysglycemic regions, providing a clearer understanding of the model’s performance across different glucose conditions. This detailed breakdown highlights the model’s strengths and identifies areas for improvement in managing varying glucose states. Precision and recall offer valuable insights: high precision indicates that the model accurately predicts dysglycemia, reducing false alarms, while high recall shows that the model effectively detects dysglycemic events, minimizing missed occurrences. Tables 5 and 6 present these metrics for the OhioT1DM and AZT1D datasets, comparing the performance of the basic CNN-LSTM model and GLIMMER. These metrics, along with RMSE and MAE, provide a comprehensive assessment of the model’s reliability and effectiveness in supporting diabetes management and patient safety.

In the OhioT1DM dataset, GLIMMER significantly improves hypoglycemia detection, increasing recall from 16% to 42%, meaning it captures more true low blood sugar events, which is vital for patient safety. The F1 score for hypoglycemia rises from 35% to 44%, reflecting a better balance between detecting true events and minimizing false positives. For hyperglycemia, GLIMMER also improves recall by 10%, from 78% to 86%, ensuring more high blood sugar episodes are detected. With a 5% improvement in precision, it reduces false alarms, making the model more reliable and user-friendly in managing glucose levels.

Table 5: Performance comparison between GLIMMER and the basic CNN-LSTM model in different glucose regions of the OhioT1DM dataset with PH = 60 minutes.

Metrics	GLIMMER				Basic CNN-LSTM			
	Normal	Dysglycemia	Hyperglycemia	Hypoglycemia	Normal	Dysglycemia	Hyperglycemia	Hypoglycemia
RMSE (mg/dL)	21.46 \pm 3.29	28.06 \pm 6.06	28.77 \pm 7.28	24.61 \pm 6.98	26.43 \pm 2.46	39.94 \pm 7.92	40.58 \pm 9.77	36.24 \pm 9.04
MAE (mg/dL)	14.43 \pm 2.14	18.54 \pm 3.18	19.12 \pm 4.05	18.45 \pm 8.22	19.54 \pm 1.90	29.33 \pm 6.03	30.00 \pm 7.61	30.41 \pm 9.21
F1 Score (%)	94.00 \pm 1.00	91.00 \pm 4.00	85.00 \pm 4.00	44.00 \pm 23.00	94.00 \pm 2.00	85.00 \pm 5.00	78.00 \pm 6.00	35.00 \pm 19.00
Recall (%)	100.00 \pm 0.00	100.00 \pm 0.00	86.00 \pm 5.00	42.00 \pm 29.00	100.00 \pm 0.00	100.00 \pm 0.00	78.00 \pm 7.00	16.00 \pm 21.00
Precision (%)	89.00 \pm 2.00	84.00 \pm 6.00	83.00 \pm 5.00	46.00 \pm 23.00	88.00 \pm 3.00	74.00 \pm 8.00	79.00 \pm 9.00	34.00 \pm 27.00

Table 6: Performance Comparison between GLIMMER and the basic CNN-LSTM model in different glucose regions of the AZT1D dataset with PH = 60 minutes.

Metrics	GLIMMER				Basic CNN-LSTM			
	Normal	Dysglycemia	Hyperglycemia	Hypoglycemia	Normal	Dysglycemia	Hyperglycemia	Hypoglycemia
RMSE (mg/dL)	19.85 \pm 3.18	31.63 \pm 6.15	31.75 \pm 9.41	41.69 \pm 21.73	23.63 \pm 4.52	46.42 \pm 10.55	46.82 \pm 13.40	57.82 \pm 21.75
MAE (mg/dL)	13.99 \pm 2.51	22.86 \pm 4.68	23.43 \pm 8.95	36.15 \pm 20.69	17.95 \pm 4.04	37.28 \pm 9.43	37.97 \pm 13.09	54.89 \pm 22.32
F1 Score (%)	96.00 \pm 1.00	82.00 \pm 11.00	74.00 \pm 9.00	22.00 \pm 20.00	97.00 \pm 3.00	58.00 \pm 25.00	54.00 \pm 21.00	11.00 \pm 13.00
Recall (%)	100.00 \pm 0.00	100.00 \pm 0.00	73.00 \pm 5.00	13.00 \pm 20.00	100.00 \pm 0.00	100.00 \pm 0.00	48.00 \pm 25.00	2.00 \pm 5.00
Precision (%)	93.00 \pm 3.00	71.00 \pm 14.00	72.00 \pm 9.00	47.00 \pm 26.00	94.00 \pm 5.00	45.00 \pm 24.00	68.00 \pm 18.00	49.00 \pm 37.00

In the AZT1D dataset, GLIMMER shows notable gains in both recall and precision for hypoglycemia detection. Recall improves from 2% to 13%, meaning it catches more low blood sugar events, while precision rises from 34% to 47%, reducing unnecessary alerts. For hyperglycemia, GLIMMER’s recall jumps from 48% to 73%, a 52% improvement, allowing it to detect more high glucose events. The model also enhances precision by 15%, ensuring better accuracy in its predictions, making it a more effective tool for managing critical dysglycemic events.

To better interpret the improvements presented in Tables 5 and 6, Figure 7 highlights the advantages of GLIMMER over the baseline CNN-LSTM model, particularly in clinically significant regions. The figure demonstrates that GLIMMER more accurately captures blood glucose fluctuations—especially during post-meal spikes—due to the integration of a targeted loss function designed to emphasize errors in dysglycemic ranges. These improvements are clinically meaningful, as they may allow for earlier detection of postprandial hyperglycemia and more timely corrective action. Such capability addresses a critical limitation in current AID systems, which often react too late or deliver insufficient boluses after meals. The model’s consistent performance across both the OhioT1DM and AZT1D datasets further supports its robustness and generalizability.

7. Discussion

Our experiments demonstrated that GLIMMER achieves superior performance and accuracy as a predictive model, surpassing the state-of-the-art models. Additionally, CEG analysis validated its reliability in detecting and forecasting dysglycemic events. Recent work by Annuzzi et al. [48] explored how certain features affect blood glucose prediction using XAI (Explainable AI) methodologies. They reported an RMSE of 24.47 ± 4.27 on the AI4PG dataset, with a prediction horizon of 60 minutes. Their model depends on detailed data inputs, including preprandial blood glucose levels, insulin dosages, and meal-related factors such as energy intake, macro-nutrients, glycemic index, and glycemic load. However, we note that in real-world scenarios, obtaining these details can be challenging, as it often requires manual logging of meal and nutritional information. GLIMMER, on the other hand, achieves strong predictions using only features like CGM data, bolus and basal insulin levels, and carbohydrate amounts that are commonly obtained in automated insulin delivery systems by default. As a result, GLIMMER does not impose any additional data collection burden on the patients beyond what the standard of care requires.

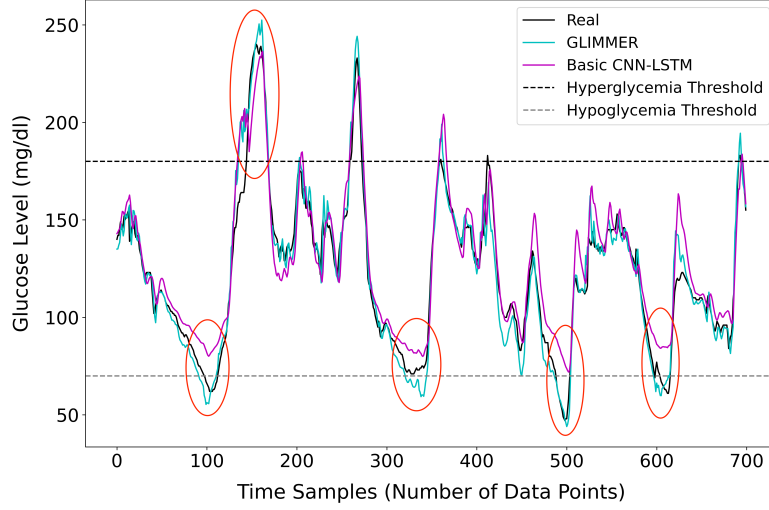


Figure 7: Forecasting comparison between GLIMMER and the basic CNN-LSTM model. The solid black line shows the real CGM values for patient 552 from the OhioT1DM test dataset (700 data points at 5-minute intervals). The dashed black and gray lines indicate hyperglycemia (180 mg/dL) and hypoglycemia (70 mg/dL) thresholds. The red circles highlight regions with noticeable prediction errors, where GLIMMER achieves smaller deviations from the real CGM values than the basic CNN-LSTM model, particularly in critical glucose ranges.

Although similar works, such as that of Cichosz et al. (2021) [49], introduced the concept of error-weighted glucose prediction, GLIMMER advances this approach in several important ways. Rather than relying on fixed penalty weights, our method employs a genetic algorithm to learn data-driven weights for a custom loss function, enabling more adaptive error prioritization. GLIMMER also places explicit emphasis on minimizing prediction errors in clinically significant dysglycemic regions—hypoglycemia and hyperglycemia—where accurate forecasts are most critical. In terms of architecture, we leverage a CNN-LSTM model tailored to capture the temporal dynamics and multivariate structure of glucose data, offering greater representational power compared to shallow feed-forward networks used in earlier work. This is further enhanced by domain-specific feature engineering, designed to reflect physiological patterns underlying glucose fluctuations.

In light of the contributions presented, some limitations still warrant discussion. While GLIMMER shows improvement in F1 score, precision, and recall over the baseline CNN-LSTM model, its hypoglycemia prediction performance is still limited. One reason for this limitation is the sparsity of hypoglycemic events in both the OhioT1DM and AZT1D datasets used in this study. The scarcity of these events means the algorithm has fewer examples from which to learn hypoglycemia patterns effectively. Additionally, we were unable to compare GLIMMER to other models on the AZT1D dataset because the source codes for these methods are not publicly available. In future work, we plan to implement and evaluate additional models to achieve a more comprehensive assessment.

The performance of glucose prediction models like GLIMMER is inherently dependent on the accuracy and reliability of glucose sensing technologies. Currently, CGMs represent the clinical standard, providing near real-time interstitial glucose readings with steadily improving accuracy and usability [50]. CGMs remain central to most automated insulin delivery systems and were the primary input source in our study. However, they are still constrained by physiological lag time, sensor calibration needs, and signal noise. Emerging biosensing methods—such as sweat-based detection [51], breath analysis [52], reverse iontophoresis [53], and optical spectroscopy [54]—offer potential for non-invasive or faster sensing, but most remain experimental and lack the clinical validation required for integration into routine care. Improvements in biosensor technology could reduce latency, improve measurement fidelity, and ultimately enhance the quality and reliability of glucose forecasts. As these innovations mature, they may open new opportunities to refine models like GLIMMER or extend them to entirely new care settings.

Despite GLIMMER’s reliance on a CNN-LSTM structure, the underlying methodologies introduced, such as the custom loss function and optimization algorithm, are generalizable and can be applied to other architectures. As part of future work, we plan to design more advanced forecasting models, such as attention-based or transformer-based networks, to explore GLIMMER’s performance within more complex time-series frameworks. We also aim to extend the prediction horizon up to 120 minutes and incorporate longer-term features to enhance accuracy over extended periods. As illustrated in Figure 1, integrating GLIMMER with automated insulin delivery systems and deploying a companion smartphone application could enable real-time alerts for patients and clinicians, providing two-hour-ahead blood glucose projections and supporting early intervention. Additionally, we plan to expand the AZT1D dataset from 25 to 100 patients, further strengthening the generalizability of our findings and enabling richer model development and evaluation.

8. Conclusion

In this paper, we introduce **GLIMMER**, a machine learning algorithm with a custom loss function designed to improve blood glucose predictions and create more reliable opportunities for behavioral and medical interventions in type 1 diabetes management. Our contribution focuses on accurate predictions in dysglycemic regions, where patients face the greatest risk and where existing models often underperform. By combining carefully selected input features with a loss function fine-tuned through a genetic algorithm, GLIMMER achieves substantial improvements over state-of-the-art models, reducing RMSE by 23% and MAE by 31% on the OhioT1DM dataset. We also collected and leveraged a new real-world dataset comprising CGM records and insulin delivery events from 25 patients with T1D, validating GLIMMER’s generalizability and creating a valuable resource for future research. These findings demonstrate that GLIMMER can be integrated into automated insulin delivery systems and smartphone applications, supporting patients and clinicians in managing T1D more effectively and preventing dangerous glycemic events.

9. Acknowledgment

This work was supported in part by the Mayo Clinic and Arizona State University Alliance for Health Care Collaborative Research Seed Grant Program under Award Number ARI-320598. Any opinions, findings, conclusions, or recommendations expressed in this material are those of the authors and do not necessarily reflect the views of the funding organization.

References

- [1] M. A. Atkinson, G. S. Eisenbarth, A. W. Michels, Type 1 diabetes, *The lancet* 383 (9911) (2014) 69–82.
- [2] D. Control, C. T. of Diabetes Interventions, C. D. S. R. Group, Intensive diabetes treatment and cardiovascular disease in patients with type 1 diabetes, *New England Journal of Medicine* 353 (25) (2005) 2643–2653.
- [3] M. Karvonen, M. Viik-Kajander, E. Moltchanova, I. Libman, R. LaPorte, J. Tuomilehto, Incidence of childhood type 1 diabetes worldwide. diabetes mondiale (diamond) project group., *Diabetes care* 23 (10) (2000) 1516–1526.
- [4] S. J. Guo, H. Shao, Growing global burden of type 1 diabetes needs multitiered precision public health interventions, *The Lancet Diabetes & Endocrinology* 10 (10) (2022) 688–689.
- [5] A. Z. Woldaregay, E. Årsand, S. Walderhaug, D. Albers, L. Mamykina, T. Botsis, G. Hartvigsen, Data-driven modeling and prediction of blood glucose dynamics: Machine learning applications in type 1 diabetes, *Artificial intelligence in medicine* 98 (2019) 109–134.
- [6] J. L. Parkes, S. L. Slatin, S. Pardo, B. H. Ginsberg, A new consensus error grid to evaluate the clinical significance of inaccuracies in the measurement of blood glucose., *Diabetes care* 23 (8) (2000) 1143–1148.
- [7] M. Jaloli, M. Cescon, Long-term prediction of blood glucose levels in type 1 diabetes using a cnn-lstm-based deep neural network, *Journal of diabetes science and technology* 17 (6) (2023) 1590–1601.
- [8] M. Marigliano, C. Piona, V. Mancioppi, E. Morotti, A. Morandi, C. Maffei, Glucose sensor with predictive alarm for hypoglycaemia: Improved glycaemic control in adolescents with type 1 diabetes, *Diabetes, Obesity and Metabolism* 26 (4) (2024) 1314–1320.
- [9] M. Vettoretti, G. Cappon, A. Facchinetti, G. Sparacino, Advanced diabetes management using artificial intelligence and continuous glucose monitoring sensors, *Sensors* 20 (14) (2020) 3870.
- [10] S. Templer, Closed-loop insulin delivery systems: past, present, and future directions, *Frontiers in Endocrinology* 13 (2022) 919942.

- [11] J. L. Sherr, L. Heinemann, G. A. Fleming, R. M. Bergenstal, D. Bruttomesso, H. Hanaire, R. W. Holl, J. R. Petrie, A. L. Peters, M. Evans, Automated insulin delivery: benefits, challenges, and recommendations. a consensus report of the joint diabetes technology working group of the european association for the study of diabetes and the american diabetes association, *Diabetes Care* 45 (12) (2022) 3058–3074.
- [12] E. Renard, M. Joubert, O. Villard, B. Dreves, Y. Reznik, A. Farret, J. Place, M. D. Breton, B. P. Kovatchev, iDCL Trial Research Group, Safety and efficacy of sustained automated insulin delivery compared with sensor and pump therapy in adults with type 1 diabetes at high risk for hypoglycemia: a randomized controlled trial, *Diabetes Care* 46 (12) (2023) 2180–2187.
- [13] S. Oviedo, J. Vehí, R. Calm, J. Armengol, A review of personalized blood glucose prediction strategies for t1dm patients, *International journal for numerical methods in biomedical engineering* 33 (6) (2017) e2833.
- [14] T. Zhu, K. Li, P. Herrero, J. Chen, P. Georgiou, A deep learning algorithm for personalized blood glucose prediction., in: *KDH@IJCAI*, 2018, pp. 64–78.
- [15] L. L. Del Giudice, A. Piersanti, C. Göbl, L. Burattini, A. Tura, M. Morettini, Availability of open dynamic glycemc data in the field of diabetes research: A scoping review, *Journal of Diabetes Science and Technology* (2025) 19322968251316896.
- [16] T. Zhu, K. Li, P. Herrero, P. Georgiou, Personalized blood glucose prediction for type 1 diabetes using evidential deep learning and meta-learning, *IEEE Transactions on Biomedical Engineering* 70 (1) (2022) 193–204.
- [17] S. Khamesian, A. Arefeen, B. M. Thompson, M. A. Grando, H. Ghasemzadeh, Aztd: A real-world dataset for type 1 diabetes, *arXiv preprint arXiv:2506.14789* (2025).
- [18] P. Shroff, A. Arefeen, H. Ghasemzadeh, Glucoseassist: Personalized blood glucose level predictions and early dysglycemia detection, in: *2023 IEEE 19th International Conference on Body Sensor Networks (BSN)*, IEEE, 2023, pp. 1–4.
- [19] A. Arefeen, S. Fessler, C. Johnston, H. Ghasemzadeh, Forewarning postprandial hyperglycemia with interpretations using machine learning, in: *2022 IEEE-EMBS International Conference on Wearable and Implantable Body Sensor Networks (BSN)*, IEEE, 2022, pp. 1–4.
- [20] G. Keren, B. Schuller, Convolutional rnn: an enhanced model for extracting features from sequential data, in: *2016 International Joint Conference on Neural Networks (IJCNN)*, IEEE, 2016, pp. 3412–3419.
- [21] K. Li, J. Daniels, C. Liu, P. Herrero, P. Georgiou, Convolutional recurrent neural networks for glucose prediction, *IEEE journal of biomedical and health informatics* 24 (2) (2019) 603–613.
- [22] Z. Li, F. Liu, W. Yang, S. Peng, J. Zhou, A survey of convolutional neural networks: analysis, applications, and prospects, *IEEE transactions on neural networks and learning systems* 33 (12) (2021) 6999–7019.
- [23] L. R. Medsker, L. Jain, et al., Recurrent neural networks, *Design and Applications* 5 (64-67) (2001) 2.
- [24] S. Hochreiter, J. Schmidhuber, Long short-term memory, *Neural computation* 9 (8) (1997) 1735–1780.
- [25] A. Aliberti, I. Pupillo, S. Terna, E. Macii, S. Di Cataldo, E. Patti, A. Acquaviva, A multi-patient data-driven approach to blood glucose prediction, *IEEE Access* 7 (2019) 69311–69325.
- [26] S. A. Billings, *Nonlinear system identification: NARMAX methods in the time, frequency, and spatio-temporal domains*, John Wiley & Sons, 2013.
- [27] Q. Sun, M. V. Jankovic, L. Bally, S. G. Mougiakakou, Predicting blood glucose with an lstm and bi-lstm based deep neural network, in: *2018 14th symposium on neural networks and applications (NEUREL)*, IEEE, 2018, pp. 1–5.
- [28] H. Butt, I. Khosa, M. A. Iftikhar, Feature transformation for efficient blood glucose prediction in type 1 diabetes mellitus patients, *Diagnostics* 13 (3) (2023) 340.
- [29] M. Zhang, K. B. Flores, H. T. Tran, Deep learning and regression approaches to forecasting blood glucose levels for type 1 diabetes, *Biomedical Signal Processing and Control* 69 (2021) 102923.
- [30] T. El Idrissi, A. Idri, Deep learning for blood glucose prediction: Cnn vs lstm, in: *Computational Science and Its Applications–ICCSA 2020: 20th International Conference, Cagliari, Italy, July 1–4, 2020, Proceedings, Part II 20*, Springer, 2020, pp. 379–393.
- [31] S. Mirshekarian, H. Shen, R. Bunescu, C. Marling, Lstms and neural attention models for blood glucose prediction: Comparative experiments on real and synthetic data, in: *2019 41st annual international conference of the IEEE engineering in medicine and biology society (EMBC)*, IEEE, 2019, pp. 706–712.
- [32] L. Yang, T. L. J. Ng, B. Smyth, R. Dong, Htm: Hierarchical transformer-based multi-task learning for volatility prediction, in: *Proceedings of The Web Conference 2020*, 2020, pp. 441–451.
- [33] K. Plis, R. C. Bunescu, C. Marling, J. Shubrook, F. Schwartz, A machine learning approach to predicting blood glucose levels for diabetes management., in: *AAAI Workshop: Modern Artificial Intelligence for Health Analytics*, no. 31, 2014, pp. 35–39.
- [34] E. I. Georga, V. C. Protopappas, D. Ardigo, M. Marina, I. Zavaroni, D. Polyzos, D. I. Fotiadis, Multivariate prediction of subcutaneous glucose concentration in type 1 diabetes patients based on support vector regression, *IEEE journal of biomedical and health informatics* 17 (1) (2012) 71–81.
- [35] W. Lu, J. Li, Y. Li, A. Sun, J. Wang, A cnn-lstm-based model to forecast stock prices, *Complexity* 2020 (1) (2020) 6622927.
- [36] M. Alhussein, K. Aurangzeb, S. I. Haider, Hybrid cnn-lstm model for short-term individual household load forecasting, *Ieee Access* 8 (2020) 180544–180557.
- [37] Q. Wu, F. Guan, C. Lv, Y. Huang, Ultra-short-term multi-step wind power forecasting based on cnn-lstm, *IET Renewable Power Generation* 15 (5) (2021) 1019–1029.
- [38] A. Chico, J. Moreno-Fernández, D. Fernández-García, E. Solá, The hybrid closed-loop system tandem t: slim x2™ with control-iq technology: expert recommendations for better management and optimization, *Diabetes Therapy* 15 (1) (2024) 281–295.
- [39] M. Mitchell, *An introduction to genetic algorithms*, MIT press, 1998.

- [40] Y. Jin, A comprehensive survey of fitness approximation in evolutionary computation, *Soft computing* 9 (1) (2005) 3–12.
- [41] S. Khamesian, H. Malek, Hybrid self-attention neat: a novel evolutionary self-attention approach to improve the neat algorithm in high dimensional inputs, *Evolving Systems* 15 (2) (2024) 489–503.
- [42] C. Marling, R. Bunescu, The ohiot1dm dataset for blood glucose level prediction: Update 2020, in: *CEUR workshop proceedings*, Vol. 2675, NIH Public Access, 2020, p. 71.
- [43] A. Zheng, A. Casari, *Feature engineering for machine learning: principles and techniques for data scientists*, " O'Reilly Media, Inc.", 2018.
- [44] P. J. Brockwell, R. A. Davis, *Introduction to time series and forecasting*, Springer, 2002.
- [45] J. J. Dylag, Machine learning based prediction of glucose levels in type 1 diabetes patients with the use of continuous glucose monitoring data, *arXiv preprint arXiv:2302.12856* (2023).
- [46] W. L. Clarke, D. Cox, L. A. Gonder-Frederick, W. Carter, S. L. Pohl, Evaluating clinical accuracy of systems for self-monitoring of blood glucose, *Diabetes care* 10 (5) (1987) 622–628.
- [47] E. I. Georga, V. C. Protopappas, D. Polyzos, D. I. Fotiadis, A predictive model of subcutaneous glucose concentration in type 1 diabetes based on random forests, in: *2012 Annual International Conference of the IEEE Engineering in Medicine and Biology Society*, IEEE, 2012, pp. 2889–2892.
- [48] G. Annuzzi, A. Apicella, P. Arpaia, L. Bozzetto, S. Criscuolo, E. De Benedetto, M. Pesola, R. Prevete, Exploring nutritional influence on blood glucose forecasting for type 1 diabetes using explainable ai, *IEEE journal of biomedical and health informatics* (2023).
- [49] S. L. Cichosz, T. Kronborg, M. H. Jensen, O. Hejlesen, Penalty weighted glucose prediction models could lead to better clinically usage, *Computers in Biology and Medicine* 138 (2021) 104865.
- [50] D. Rodbard, Continuous glucose monitoring: A review of successes, challenges, and opportunities, *Diabetes Technology & Therapeutics* 18 (Suppl. 2) (2016) S3–S13. doi:10.1089/dia.2015.0417.
- [51] W. Gao, S. Emaminejad, H. K. Nyein, S. Challa, K. Chen, A. H. Peck, H. M. Fahad, H. Ota, H. Shiraki, D. Kiriya, D. Lien, G. A. Brooks, R. W. Davis, A. Javey, Fully integrated wearable sensor arrays for multiplexed in situ perspiration analysis, in: *Nature*, Vol. 529, 2016, pp. 509–514. doi:10.1038/nature16521.
- [52] J. Yan, D. Zhang, X. Zhang, Y. Jiang, Z. Ye, Design and evaluation of a portable non-invasive glucose monitor based on breath analysis, *IEEE Sensors Journal* 14 (6) (2014) 2067–2073. doi:10.1109/JSEN.2013.2292285.
- [53] R. O. Potts, J. van Heerden, Glucose monitoring by reverse iontophoresis, *Diabetes Technology & Therapeutics* 4 (1) (2002) 105–114. doi:10.1089/152091502753364617.
- [54] S. Liakat, W. Cai, Q. Yu, Y. He, M. Bourham, A. Fasoula, W.-Y. Tseng, P. Salama, C. Apblett, R. Dietz, M. Samant, A. El-Badry, T. Dinardo, J. Ferguson, G. Ray, C. Lehnick, Non-invasive glucose monitoring using optical spectroscopy, *Instrumentation Science & Technology* 42 (3) (2014) 273–287. doi:10.1080/10739149.2013.855058.